34th Annual International Conference of the IEEE EMBS
San Diego, California USA, 28 August - 1 September, 2012

Intradermal Needle-Free Powdered Drug Injection by a Helium-Powered Device

John Liu, N. Catherine Hogan, and Ian W. Hunter*

***Abstract*—We present a new method for needle-free powdered drug injection via a bench-top gas-powered device. This injector provides an alternative method of vaccine delivery to address the cold chain problem—the cost and risk of transporting temperature sensitive vaccines to developing countries. The device houses interchangeable nozzle inserts to vary orifice geometries and is capable of delivering polymer beads (1-5 μm diameter) into the dermal layer of porcine tissue. Results for injection shape and injection depth versus nozzle orifice diameter demonstrate the device's controllability.**

I. Introduction

Vaccine immunization saves more than three million lives worldwide each year [1] and is considered to be one of the most cost effective measures of addressing disease on the global scale. Over 100 million children below the age of one are immunized against measles, polio, and other diseases [2,3]. There remain areas for great improvement, namely the cold chain—the temperature controlled supply system of vaccines stored at temperatures of 2-8 °C—which is one of the most vulnerable aspects of vaccine delivery for the developing world and costs an estimated 200-300 million dollars a year [4]. Numerous studies across different countries show frequent refrigeration malfunction leading to drug waste and vaccination using compromised vaccines [5].

To alleviate the problems currently associated with the cold chain, different approaches have been investigated. Efforts such as the WHO's drug diagnosis and new refrigeration and temperature monitoring technologies have offered some improvement [6]. Lyophilization of vaccines has improved the shelf life of many formulations but lyophilized drug still needs to be refrigerated. Reformulating drugs to be thermostable between the temperatures of freezing and 45°C by methods such as spray drying and spray freeze drying are currently being developed. In particular, a recent study showed spray-dried formulations of the Hepatitis B vaccine were stable for at least 24 months at 37 °C [7].

In the context of global vaccinations, jet injection has been a promising technology because of its elimination of "needle phobia," increased patient compliance, and elimination of sharps injury and sharps disposal [4]. Most current needle-free injection systems use aqueous solutions, which require reconstitution of the drug. Because reconstituted drug is thermally unstable, unused reconstituted drugs must be disposed of after 24 hours, leading to drug wastage [8]. If powdered vaccines can be delivered directly, there is no need for diluent and reconstitution, further cutting costs in storage, transportation, and human training and error.

To date, few powder injection systems have been developed. A helium-powered needle-free technology [9] is able to perform epidermal powder immunization [10]. However, because particle penetration is governed by the ballistics of individual particles, constraints exist on the size and density of each particle to achieve momentum density sufficient for penetration. Because of these constraints, standard pharmaceutical formulation techniques may need to be modified [11] and this technology may not be ideal in situations where financial resources are limited. Nasal powder vaccines are also being developed for aerosol delivery, but there are still constraints on sizes of the actuated droplet and medicinal agent for proper placement of the deposited drug and avoidance of inflammatory responses [12].

This paper presents a new method of powdered drug delivery. We demonstrate that a simple and inexpensive bench-top helium-powered device is capable of delivering particles into porcine tissue to depths of 260 to 1125 μm. Because penetration of the powder is not dependent on the ballistics of the particle but the jet mechanics of the carrying gas, there are fewer restrictions on the physical parameters of the delivered particle. Further development of this type of technology could provide a platform for the delivery of a variety of powdered drug formulations.

II. Material & Methods

A. Bench-top Setup

The bench top setup (Fig. 1) is composed of a high-pressure stainless steel solenoid valve (Parker model 71216) connected to a tank carrying industrial-grade helium (Airgas HE40) by a smooth-bore stainless steel gas hose (Unisource 4TSC-11-11-36.0) and outfitted pressure regulator (Airgas E13-N115H). A pressure sensor is attached between the pressure regulator (Omega model PX303-4KG5V) and hose to determine the applied pressure at the nozzle.

B. Electronics

A timer circuit is used to release a 15 ms pulse at 24 V from the power supply to energize the solenoid valve.

C. Nozzle

The outside housing of a carbon steel compression fitting (Parker Yor-Lok) houses one acrylic disk and a machined aluminum piece to mate to the surface of the inside of the compression fitting (Fig. 2a). When the pieces are assembled and tightened in the compression fitting, the acrylic disk and

*Research is supported by the NSF Graduate Research Fellowship and Sanofi S.A., Paris, France.

J. Liu, N. C. Hogan, and I.W. Hunter are with the Bioinstrumentation Laboratory, Department of Mechanical Engineering, Massachusetts Institute of Technology, Cambridge, MA 02139 USA (e-mail: johnhliu@mit.edu).

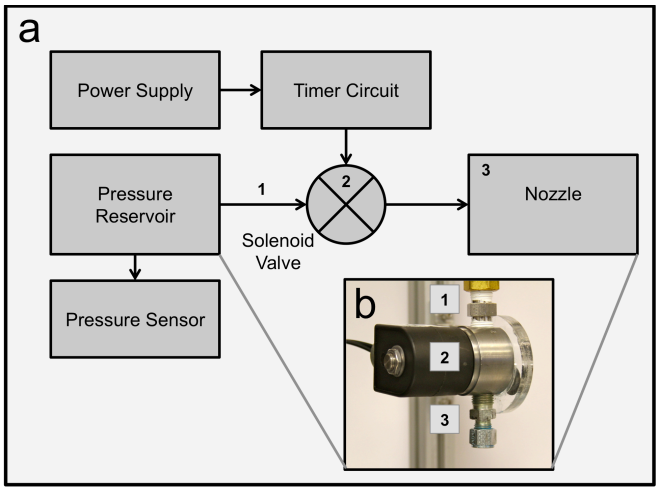

Figure 1. a) Block diagram of the bench-top powder injector. b) photograph of the device. Gas flows from the gas tank through the hose (1) to the solenoid valve (2) and to the nozzle (3).

aluminum piece are compressed together to form a gas-tight seal in the fitting, resulting in a composite nozzle that can house acrylic disks of different orifice geometries. Because of the speed and ease of use of laser machining, manufacturing acrylic disks lends itself well to rapid prototyping. 1.7 mm thick acrylic was laser machined to yield orifice diameters ranging from 20 to 200 µm (Fig. 2b).

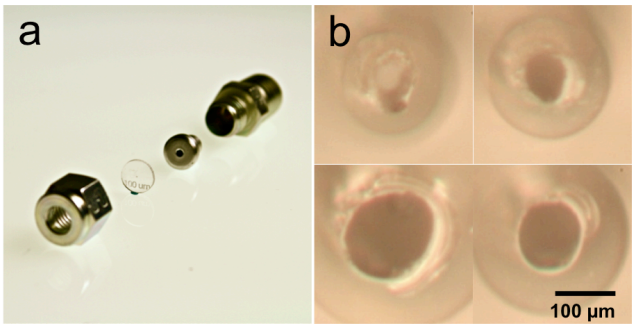

Figure 2. Photographs of the nozzle assembly. (a) The outer housing of the compression fitting houses an acrylic disk and a custom-machined aluminum piece to mate to the compression fitting surface. The result is an assembly capable of housing (b) acrylic disks of different diameter orifices (here shown clockwise starting from upper left: 40, 60, 100, 150 µm) at a high pressure.

D. Powder

Blue polymer microspheres (1-5 µm diameter, 1.3 g/cc) were purchased from Cospheric LLC for ready visualization. By size and density, these microspheres are on the order of common lyophilized vaccines [11,13].

E. In Vitro Injections

Post mortem porcine tissue was obtained through the MIT Tissue Harvest Program using procedures approved by the IUCAC and in accordance with the NIH Guide for the Use and Care of Laboratory Animals. Tissue was harvested from the abdomen of Yorkshire pigs (approximately 6 months) immediately after euthanasia and included subcutaneous fat and skin. The tissue was trimmed, immediately vacuum sealed, and stored at -80 °C. Prior to injection, each sample was thawed at 4°C and equilibrated to room temperature. For each injection, approximately 1 mg of powder was loaded into the nozzle, which was placed in direct contact with the tissue sample.

To determine the volume of gas ejected in a single injection, the nozzle setup was placed in a sealed Buchner flask, and the difference in pressure within the chamber before and after an injection trial was measured using a pressure sensor (Vernier GPS-BTA). Injections were also recorded using a high-speed CMOS video camera (Phantom v9, Vision Research) fitted with a 65 mm macro photo lens (Canon MP-E 65). The injections were captured at a resolution of 1440 x 720 and a frame rate of 1016 fps.

After injection, tissue was placed in plastic containers (22 mm x 22 mm x 18 mm) containing optimal cutting temperature compound (Tissue-Tek OCT Compound) and frozen in liquid nitrogen. Tissue slices 15 µm thick were then successively removed from each sample using a Vibratome Ultra Pro 5000 cryostat. A Canon EOS-7D camera, fitted with a 65 mm macro photo lens (Canon MP-E 65) was used to photograph the tissue after removal of each section, yielding a series of photos that when compiled imaged through the entire block of tissue. Image processing and 3D reconstruction of the injection was performed in MATLAB.

III. Results

Upon release of high-pressure gas into the nozzle, the gas entrains the powder, forming a jet consisting of gas and powder that punctures the tissue. The jet once it has punctured the stratum corneum may produce two effects. In the first case, an erosion hole is created but powder is not dispersed through the tissue (Fig. 3a) while in the second case, an erosion hole is created followed by dispersion of drug into the tissue (Fig. 3b). For the purpose of analysis, the former case is not considered to represent a successful injection. As such injection profiles have been quantified using two measurements: D_h the depth of the erosion hole, and D_d the depth of powder dispersion.

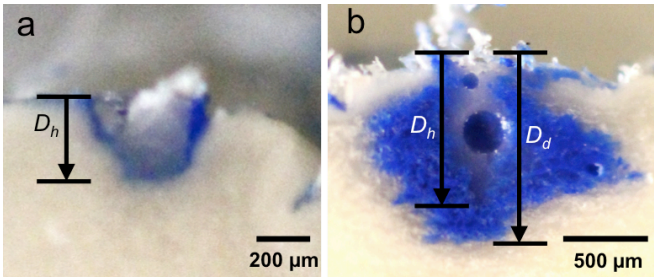

Figure 3. Representative tissue midline cross-sections of two types of injection trials: (a) an erosion hole with no dispersion in tissue which is considered unsuccessful and (b) an erosion hole with powder dispersion considered to be successful. Frozen OCT in the erosion hole appears has a bluish white appearance. In (b) an air bubble in the frozen OCT appears as a darkened hole in the middle of the erosion hole.

A. Shape of Powder Injection

Reconstruction of successful powder injections into porcine tissue revealed that the injection profiles were quite varied. The most common shapes observed in successful injections could be classified as an upside down cone (Fig. 4a), an upright cone (Fig. 4b), or a sphere (Fig. 4c).

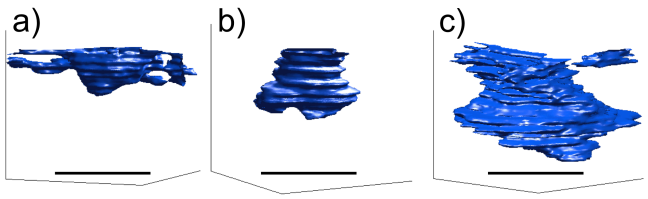

Figure 4. 3D MATLAB reconstructions of the tissue injection shape. Three primary shapes were observed (a) upside down cone, (b) right side cone, and (c) sphere. The powder dispersion depth corresponding to each 3D reconstruction is 441, 810, and 1125 μm, respectively (scale bars = 1 mm).

These injection shapes are associated with the development of the actual injection. An upside down cone was observed with the most shallow of injections, whereas the sphere was commonly observed with the deepest of injections. Fluid and powder dispersion within tissue originates from what can be thought of as a point source of radially outward flowing fluid [14]. As dispersion depth increases, the point source also increases in depth and a greater section of the sphere is realized; in a shallow injection, this point source can be thought of as resting on the surface, hence only the bottom part of the sphere is realized. The right side cone—the intermediate stage—may be thought of as an underdeveloped sphere, and thus the shape more closely resembles a right side cone. These observations are similar to those for needle-free injections using aqueous solutions. While helium gas is a highly compressible fluid these results are consistent with the point-source hypothesis for incompressible fluid injection.

B. *Tissue Inflation*

In successful injections, it was often observed that the helium inflated the tissue sample. Fig. 5a shows a time-lapse series of photographs demonstrating tissue inflation at 0.05 s after the start of injection and deflation within 1.22 s. The volume of helium delivered in an injection was found to increase with pressure, from 4.9 mL at 2.1 MPa to 10.4 mL at 10.2 MPa. Because of helium's high diffusivity in tissue and low solubility in blood [15], we conjecture that injection of helium into the upper layers of tissue poses little risk of inducing gas embolism [16]. However, there may still be a risk of inducing cutaneous decompression sickness [16] in the local region of injection. *In vivo* animal experiments need to be performed to assess the health effects of helium injection into the dermis.

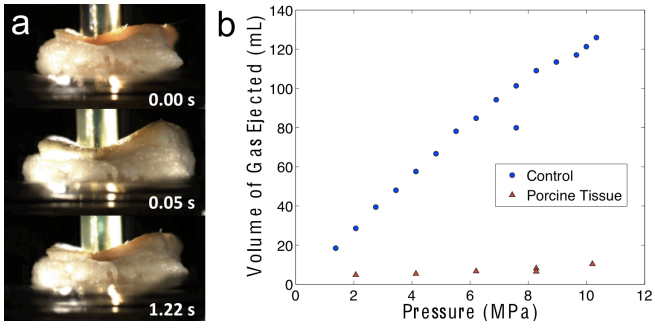

Figure 5. (a) Time-lapse photograph series of pre-, mid-, and post-injection. Note the inflation in the second picture (0.05 s) and deflation in the third (1.22 s). (b) Volume of gas ejected from the nozzle (mL) as a function of applied pressure (MPa). Ejections into air served as the control.

C. *Depth of Injection versus Nozzle Diameter*

In general, we observed a correlation of both erosion hole depth and dispersion depth with increasing nozzle orifice diameter (Fig. 6). The results of single trials performed at two pressure settings (Trial 1: 8.9-9.0 MPa [n = 16] and Trial 2: 10.1 MPa [n = 10]) have been plotted (Fig. 6). Given the observation that the acrylic disk orifices generally expanded under the applied pressure of an injection, average of nozzle orifice diameters before and after injections are presented. Injection success and failure is also differentiated in each data set. Average nozzle diameters for data compiled from Trial 1 and Trial 2 ranged from 33 to 173 μm and 54 to 159 μm, respectively. Fig. 6a shows erosion hole depth (D_h) versus nozzle orifice diameter: D_h ranged from 91 to 860 μm for Trial 1 and 313 to 585 μm for Trial 2. Fig. 6b shows dispersion depth (D_d) versus nozzle orifice diameter: D_d ranged from 260 to 1090 μm for Trial 1 and 441 to 1125 μm for Trial 2.

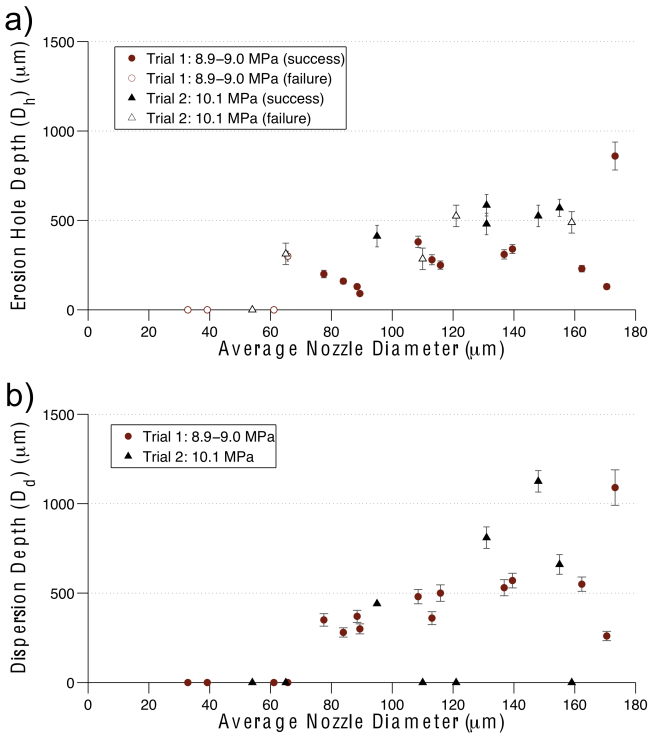

Figure 6. Erosion hole depth, D_h, and dispersion depth, D_d, are quantifiable metrics of the injection profiles of two different applied pressures: 8.9-9.0 MPa (Trial 1) and 10.1 MPa (Trial 2). (a) Dependence of D_h on average nozzle diameter at constant pressure. Data of successful injections are presented as filled in shapes, unsuccessful as unfilled. (b) Dependence of D_d on average nozzle diameter at constant pressure. The injection depth of an unsuccessful injection is considered to be zero ($D_d = 0$).

The correlation of both erosion hole depth and dispersion depth with nozzle diameter became more apparent when the data was grouped into 25 μm ranges (n = 2-4) and the respective depths averaged (Fig. 7). For an applied pressure of 8.9-9.0 MPa, trials were unsuccessful in the 25-75 μm range: erosion holes and powder dispersion were not observed in the 25-50 μm diameter range and erosion holes but not powder dispersion were observed in the 50-75 μm range. Both erosion holes and powder dispersion were observed (successful) in the 75-175 μm range.

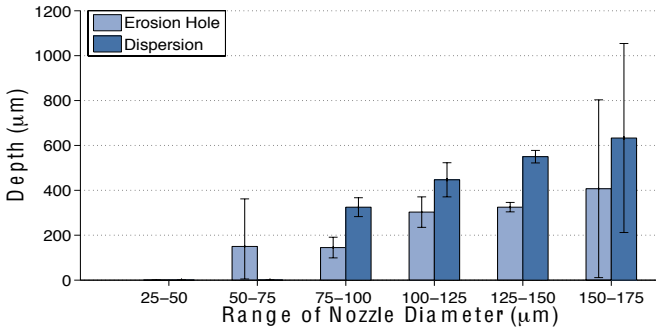

Figure 7. Depth data for 25 µm ranges of nozzle diameters at injections at 8.9-9.0 MPa of applied pressure. Depth of both erosion hole and powder dispersion generally increases with applied pressure.

IV. Discussion

For a given applied pressure, there is a general increase in erosion hole depth and dispersion depth with an increase in nozzle diameter. Both trends are consistent with the tissue mechanics theory of liquid jet penetration in tissue, which indicates that an increase in jet power (P_0),

$$P_0 = \pi D_n^2 \sqrt{\frac{p^3}{8\rho}}, \quad (1)$$

leads to an increase in injection depth, where D_n is the nozzle diameter, p is the applied pressure, and ρ is the density of the fluid [14,16]. The observation that successful injections are not observed in trials using orifices of smaller diameter (e.g. 25-75 µm in Trial 1) suggests a threshold value of power below which the jet does not disperse into the tissue.

When the two data sets are compared, a general increase in both penetration and injection depth is observed with an increase in applied pressure. However, the data in Fig. 6 suggests that the consistency of injections decreases with higher pressure; injection trials using nozzles of diameter 100-175 µm in Trial 2 yielded 43% (3/7) failed injections as opposed to 0% (0/8) failed injections in the same nozzle range in Trial 1. This may be due to the gas splash back at higher pressures, which has been observed in injections of aqueous solution and can be improved by pressure pulse shaping [17].

V. Conclusion and Future Work

The device presented in this paper offers an alternative method for the intradermal delivery of powdered drug and has the potential to be implemented with stabilized formulations of vaccines to address the cold chain problem. While the device uses a compressible fluid for jet injection, the penetration, success of injection, injection depth, and injection shape are consistent with previous results obtained using incompressible fluids (aqueous solutions).

Future experimental work will include delivering thermo-stabilized formulations of vaccines *in vivo* and exploring parameters required to optimize the bioavailability of drug. Development of an inexpensive hand-held device and an economic assessment of the use of this technology in developing countries will also be conducted.

Acknowledgment

The authors thank Bryan Ruddy and Ellen Chen for their invaluable advice in experimentation. The authors would also like to thank Adam Wahab for helpful discussion during device development.

References

[1] M. Kane, H. Lasher, "The Case for Childhood Immunization," PATH, 2002, [Online] Available: http://www.unicef.org/immunization/index_coverage.html, [Accessed March 19, 2012].

[2] The Living Proof Project, "Progress Toward Immunization: Winning the fight against deadly diseases," 2009, [Online] Available: http://www.gatesfoundation.org/livingproofproject/Documents/progress-towards-immunization.pdf, [Accessed March 19, 2012].

[3] WHO, UNICEF, World Bank, "State of the world's vaccines and immunization," 3rd ed. Geneva, World Health Organization, 2009. [Online] Available: http://whqlibdoc.who.int/publications/2009/9789241563864_eng.pdf, [Accessed March 19, 2012].

[4] E.L. Giudice and J.D. Campbell, "Needle-free vaccine delivery," *Adv. Drug Deliv Rev*., vol. 58, no. 1, pp. 68-89, April 2006.

[5] D.M. Matthias, et al., "Freezing temperatures in the vaccine cold chain: a systematic literature review," *Vaccine,* vol. 25, no. 20, pp. 3980-3986, May 2007.

[6]

[7] "Not too hot, not too cold," PATH, [Online] Available: http://www.path.org/projects/cold-chain.php [Accessed March 19, 2012].

[8] D. Chen, et al., "Thermostable formulations of a hepatitis B vaccine and a meningitis A polysaccharide conjugate vaccine produced by a spray drying method," *Vaccine*, vol. 28, no. 31, pp. 5093–5099, July 2010.

[9] Immunization Action Coalition, "Vaccines with Diluents: How to Use Them," 2011, [Online] Available: http://www.immunize.org/catg.d/p3040.pdf [Accessed March 20, 2012].

[10] Bellhouse, et al., "Method of delivering powder transdermally with needless injector," U.S. Patent 5 630 796, May 20, 1997.

[11] D. Chen, et al., "Epidermal immunization by a needle-free powder delivery technology: Immunogenicity of influenza vaccine and protection in mice," *Nat. Med.,* vol. 6, no. 10, pp. 1187-1190, Oct. 2000.

[12] A.S. Ziegler, "Needle-Free Delivery of Powdered Protein Vaccines: A New and Rapidly Developing Technique," *J. Pharm. Innov.*, vol. 3, no.3, pp. 204-213, Aug. 2008.

[13] S.S. Renteriaa, C. C. Clemensa, M.A. Croyle, "Development of a nasal adenovirus-based vaccine: Effect of concentration and formulation on adenovirus stability and infectious titer during actuation from two delivery devices," *Vaccine,* vol. 28, no. 9, pp. 2137-48, Feb. 2010.

[14] A. Clausi, et al., "Influence of Particle Size and Antigen Binding on Effectiveness of Aluminum Salt Adjuvants in a Model Lysozyme Vaccine," *J Pharm Sci.*, vol. 97, no. 12, pp. 5252-5262, Dec. 2008

[15] J. Schramm-Baxter, and S. Mitragotri, "Needle-free jet injections: dependence of jet penetration and dispersion in the skin on jet power," *Journal of Controlled Release*, vol. 97, no. 3, pp. 527-535, July 2004.

[16] S. Miles and D.E. Mackay, *Underwater Medicine*. Philadelphia: J.B. Lippincott Company, 1976.

[17] J.E. Baumgardner, et al., "Gas flux through human skin: effect of temperature, stripping, and inspired tension," *J. Appl. Physiol.*, vol. 58, no. 5, 1536-1545, May 1985.

[18] D.M. Wendell, et al., "The Effect of Jet Parameters on Jet Injection", *Proc. 28th Annual International Conference of the IEEE Engineering in Medicine and Biology Society*, 2006.

[19] J.C. Stachowiak, et al., "Dynamic control of needle-free jet injection," *Journal of Controlled Release*, vol. 135, no. 2, pp. 104-112, April 2009.